# Calculations of One-Electron Redox Potentials of Oxoiron(IV) Porphyrin Complexes

Ludovic Castro and Michael Bühl*

School of Chemistry, University of St. Andrews, North Haugh, St. Andrews, Fife, KY16 9ST, Scotland, United Kingdom

Ⓢ Supporting Information

**ABSTRACT:** Density functional theory calculations have been performed to calculate the one-electron redox potential for a series of oxoiron(IV) porphyrin complexes of the form $[(TMP)Fe^{IV}(O)(L)]$ (TMP = 5,10,15,20-tetramesitylporphyrinate). Different axial ligands were chosen (L = none, Im, $ClO_4^-$, $CH_3CO_2^-$, $Cl^-$, $F^-$, $SCH_3^-$) in order to compare the results with recent electrochemical experiments. The redox potentials were calculated with a Born−Haber cycle and the use of an internal reference, i.e. the absolute redox potential of ferrocene. Diverse methodologies were tested and show that the computed redox potentials depend strongly on the functional, the basis set, and the continuum models used to compute the solvation energies. Globally, BP86 gives better results for the geometries of the complexes than B3LYP and M06-L as well as more consistent values for the redox potentials. Although the results fit the experimental data for L = Im and L = $ClO_4^-$, the addition of the other anionic axial ligands to the oxoiron(IV) porphyrin complex strongly lowers the redox potential, which is in disagreement with experimental observations. This important discrepancy is discussed.
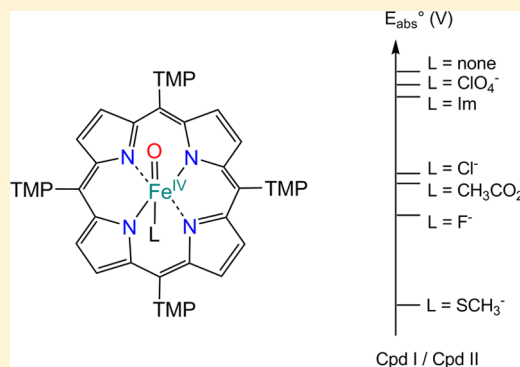
## INTRODUCTION

High-valent oxoiron(IV) porphyrin species have been implicated in the reaction mechanisms of heme enzymes such as cytochrome P450, peroxidases, and catalases.[1] During the biological catalytic cycle, the oxoiron(IV) porphyrin $\pi$-cation radical complex, Compound I (Cpd I), as well as its reduced oxoiron(IV) counterpart, Compound II (Cpd II), have been identified as important key intermediates.[2]

Heme enzymes can present a large variety of biochemical functions.[3] In cytochrome P450, Cpd I transfers its oxygen atom to a range of substrates, or it oxidizes diverse molecules or polymers by direct electron-transfer in peroxidases (see catalytic cycle in Figure 1). Thus, even if Cpd I has always been identified as the most reactive species of the catalytic cycle, its mode of action varies from one enzyme to another.

Lignin peroxidase is known to oxidize substrates of high redox potentials (RP), such as nonphenolic aromatic substrates, because of its own high RP (estimated at around 1.2 V at pH 3.0).[4] In contrast, horseradish peroxidase has a RP of 0.95 V at pH 6.3[5] and cytochrome $c$ peroxidase presents a value of 0.19 V at pH 7.[6] The reaction of a variety of methoxybenzenes presenting a large range of RP (from 0.81 to 1.76 V at pH 3.0) with diverse types of peroxidases reveals that the reaction rate increases with the RP of the enzymes.[4] Therefore, the structures of the heme enzymes define their RP, which play an important role in their reactivity toward organic substrates.

An obvious way to tune the RP is the nature of the proximal axial ligand interacting with the iron center of Cpd I. It is well-established that the nature of the sixth axial ligand plays an
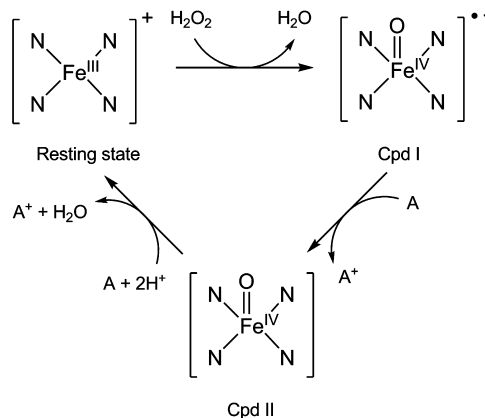


**Figure 1.** Catalytic cycle of a peroxidase (A is a substrate; N atoms from porphyrin, not shown).

important role in modifying the reactivity of Cpd I. For example, the rate constant $k$ of the epoxidation of styrene by the synthetic enzyme model complex $[(TMP^{+\bullet})Fe^{IV}(O)(L)]$ (with TMP = 5,10,15,20-tetramesitylporphyrinate) varies with the nature of the axial ligand L.[7] Indeed $k$ is found to be 7 times larger for L = $F^-$ than for L = $CH_3CO_2^-$ and almost zero for L = $ClO_4^-$. The same behavior is found for the reaction of hydrogen abstraction of alkanes by synthetic heme iron complexes.[8]
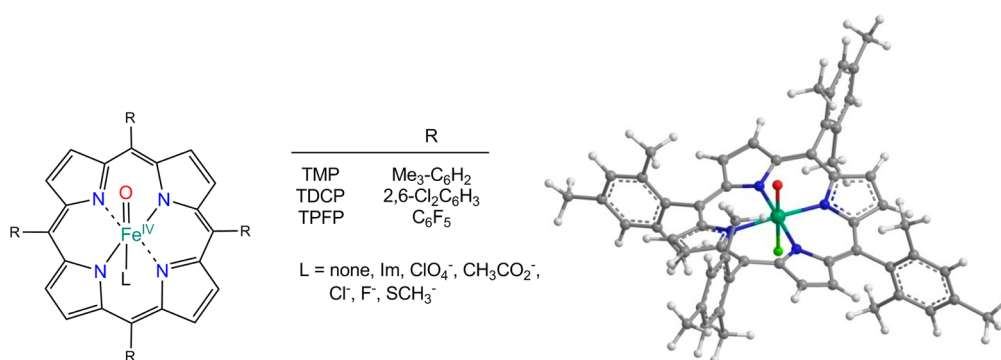
**Figure 2.** Structures of the oxoiron(IV) porphyrin complexes used in this study (left). Optimized structure of $[(TMP^{+\bullet})Fe^{IV}(O)(F^-)]$ with BP86 and B1 basis (Fe: green; O: red; F: light green; N: blue; C: gray; H: white) (right).

Recently, theoretical studies have tried to explain this axial ligand effect. Some authors state that the ligand modifies the RP of the Cpd I/Cpd II couple,[9] the proton affinity of Cpd II,[9b] the electron affinity of Cpd I[10] (which is directly related to the RP), the strength of the Fe=O bond and the FeO-H bond in Cpd II[8,11] (depending on the reactions, Cpd II can present a $Fe^{IV}$=O bond or a $Fe^{IV}$−OH bond), or the thermodynamic stability of the resting state.[12] Takahashi et al. have measured the RP of the couple $[(TMP^{+\bullet})Fe^{IV}(O)(L)]/[(TMP)Fe^{IV}(O)-(L)]$ with different axial ligands and observe that the RP undergoes a positive shift upon coordination of an anionic axial ligand (L = $Cl^-$, $F^-$, $CH_3CO_2^-$, etc.) and a negative shift upon coordination of a neutral axial ligand (L = imidazole (Im)), when L = $ClO_4^-$ is taken as the reference.[13] Moreover, the RP is shifted upward by electron-withdrawing substituents on the meso-positions of the porphyrin ring. In contrast, Dey et al., using density functional theory (DFT), have computed the electron affinities of Cpd I with a simplified porphyrin system and obtain a different order that the observed one for the RP of Takahashi et al.[9b] Indeed the electron affinity of Cpd I in solution is calculated to be 20.5 kcal/mol higher with L = Im than with L = $F^-$. Moreover, Rydberg et al. have reported a comprehensive DFT study of every step of the catalytic cycle with simplified enzyme model complexes and different axial ligands (L = $Cys^-$, $Tyr^-$, His) and the RP is found to be lower for complexes presenting negatively charged axial residues.[9a] Ogliaro et al. studied the 'push' effect of the thiolate ligand in heme systems and showed that the electron affinity of Cpd I with L = $SH^-$ is much smaller than the one with L = none, due to the combination of a field effect and quantum mechanical orbital mixing.[10a] Finally, de Visser calculated electron affinities of simplified heme systems with different axial ligands (L = Im, $Cl^-$, $SH^-$, $OH^-$) with DFT, and the results show a large decrease of the electron affinity with negatively charged ligands.[11b] These theoretical results are in apparent disagreement with the experimental observations of Takahashi et al. Thus, we decided to compute the RP of the couple $[(TMP^{+\bullet})Fe^{IV}(O)(L)]/[(TMP)Fe^{IV}(O)(L)]$ with different axial ligands (L = none, Im, $ClO_4^-$, $Cl^-$, $F^-$, $CH_3CO_2^-$, $SCH_3^-$) using three different DFT functionals (B3LYP, BP86, and M06-L) and the same conditions as in the experimental study of Takahashi et al. in order to gain more insights into this discrepancy. The paper is organized as follows: first we will present the computational methods used in this paper. Then the state-of-the-art of the computation of RP by DFT will be described. The calculated absolute redox potential (ARP) of

our reference redox couple will be reported as well as the RP of the couple of interest. A discussion will then follow.

## ■ COMPUTATIONAL SECTION

**Computational Details.** All calculations were carried out with the Gaussian 09 suite of programs.[14] Geometry optimizations were performed in the gas phase using three different DFT methods. The first functional is the hybrid B3LYP method, which incorporates Becke's three-parameter exchange functional B3 with the Lee, Yang, and Parr correlation functional LYP.[15] The second one is the generalized gradient approximation (GGA) functional BP86, which incorporates Becke's 1998 exchange functional B with Perdew's 1986 correlation functional P86.[16] The third approach is the meta-GGA functional M06-L, which is fully local, accounts implicitly for dispersion effects, and performs well for systems containing transition metals.[17] All calculations have employed the unrestricted formalism. Iron atoms were treated with the Stuttgart-Dresden relativistic effective core potential (SDD) associated with its adapted basis set.[18] Hydrogen, carbon, nitrogen, oxygen, fluorine, sulfur, and chlorine atoms were treated with the 6-31G** basis set (B1).[19] All geometries were optimized without any symmetry restrictions, and the nature of the minima was verified by analytical frequency calculations within the harmonic approximation. Single-point calculations were done on the optimized geometries with two other basis-sets for the lighter atoms: 6-311G** (B2) and 6-311++G** (B3). Thermal and entropic corrections calculated at $T = 213$ K (temperature used in the experiments of Takahashi et al.) with B1 basis were used to estimate Gibbs energies for the B2 and B3 single points. Solvation energies were evaluated by a self-consistent reaction field (SCRF) approach[20] based on accurate numerical solutions of the Poisson−Boltzmann equation.[21] Solvation calculations were carried out at the optimized gas-phase geometries with the dielectric constant of dichloromethane (solvent used in the experiments of Takahashi et al.). Different topological models were used to build the cavity around the complexes. The CPCM continuum model[22] was used with the two sets of radii Universal Force Field (UFF) and Pauling, and the SMD solvation model was used with its default settings.[23] The TMP ligand has not been simplified. The oxidant species have been computed as quartets (two single alpha electrons on the $Fe^{IV}$-centered orbitals and one single alpha electron on the $a_{2u}$ orbital of the porphyrin ring) since it has been reported as the most stable electronic state of Cpd I for horseradish peroxidase.[24] To verify that this spin state is also preferred in the TMP model systems, the oxidants were also

optimized with a doublet spin state (two single alpha electrons on the $Fe^{IV}$-centered orbitals and one single beta electron on the $a_{2u}$ orbital of the porphyrin ring). Doublet states have very similar energies as the corresponding quartets (slightly higher by around 0.2 and 0.8 kcal/mol for B3LYP and BP86 respectively). The reductant species have been computed as triplets (two single alpha electrons on the $Fe^{IV}$-centered orbitals). Optimizations were also performed with a singlet spin state. Triplet states are found more stable than singlets by around 30 kcal/mol, for both B3LYP and BP86. No significant spin contamination has been detected in all the structures computed herein. The structure of the studied complexes is shown in Figure 2. By way of example, the optimized structure of $[(TMP^{+\bullet})Fe^{IV}(O)(F^{-})]$ calculated with BP86 and the B1 basis is shown as well.

**Calculations of Redox Potentials with DFT.** Several methods exist for the theoretical prediction of standard RP in solution.[25] The most popular one uses the Born−Haber cycle presented in Figure 3. $\Delta G^{\circ}_{(g)}$ is the gas-phase Gibbs energy of
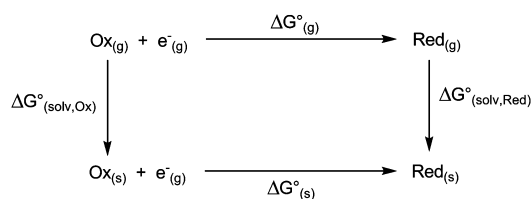


**Figure 3.** Born−Haber cycle for the computation of redox potentials.

the addition of one electron to the oxidant, which is the Cpd I complex $[(TMP^{+\bullet})Fe^{IV}(O)(L)]$ in our case. This complex is globally neutral when L is an anionic ligand and positively charged when L is a neutral ligand. The reductant, the Cpd II complex $[(TMP)Fe^{IV}(O)(L)]$, is negatively charged when L is an anionic ligand and neutral when L is a neutral ligand. It is noteworthy that $\Delta G^{\circ}_{(g)}$ is the sum of the negative calculated electron affinity, $\Delta E_{(g)}$ (i.e., a negative number if electron uptake is favorable), and the thermal and entropic contributions. In order to compute the corresponding Gibbs energy in solution, one has first to calculate the solvation energies of the oxidant and the reductant, respectively $\Delta G^{\circ}_{(solv,Ox)}$ and $\Delta G^{\circ}_{(solv,Red)}$ in Figure 3. This is commonly achieved with continuum solvation models. $\Delta G^{\circ}_{(s)}$ is eventually calculated as

$$\Delta G^{\circ}_{(s)} = \Delta G^{\circ}_{(g)} + \Delta G^{\circ}_{(solv,Red)} - \Delta G^{\circ}_{(solv,Ox)}$$

The ARP of the Ox/Red couple $E^{\circ}_{abs}$ is then defined as

$$E^{\circ}_{abs} = \frac{-\Delta G^{\circ}(s)}{nF}$$

where $n$ is the number of electrons involved in the half-reaction of interest (here $n = 1$), and $F$ is the Faraday constant ($F = 96485$ J·mol$^{-1}$·V$^{-1}$ or 23.061 kcal·mol$^{-1}$·V$^{-1}$).

In order to compare the calculated ARP with experimental RP, the computed values must be reported relative to a chosen reference. The aqueous standard hydrogen electrode (SHE) or the saturated calomel electrode (SCE) are often used as reference electrodes (RE)

$$E^{\circ}(V/RE) = E^{\circ}_{abs}(V) - E^{\circ}_{RE}(V)$$

where $E^{\circ}$ is the computed potential referenced to the reference electrode, and $E^{\circ}_{RE}$ is the absolute potential of the reference electrode.

In predictions of RPs by theoretical methods, the ARPs of the reference electrode are commonly taken from experiment. However these values vary from one experiment to the other as they depend on the solvent and the electrolyte. For the SHE, values ranging from 3.83 to 4.66 V have been reported.[26] Moreover, a liquid junction potential appears when an aqueous electrode like SCE is used in an organic solvent, which may not be reproducible in some experiments. Even nonaqueous reference electrodes present issues of reproducibility in a given solvent because of electrode surface chemistry.[27] In previous articles dealing with the calculation of RP, the usual aqueous values for SHE (4.36 and 4.43 V) have been used as reference potentials.[28] As the SCE potential is +0.24 V/SHE at 25 °C, the SCE absolute potential should be 4.60 or 4.67 V in water. Baik and Friesner chose to reference their calculated ARP to the SCE and used an incorrect value of 4.1888 V stating that the standard potential of SCE is 0.2412 V more negative, instead of positive, than the one of SHE.[29] This important mishap has been repeated by Holland et al. for the study of a set of copper complexes.[30] The consequence is that all their reported potentials are about 0.48 V higher than the effectively computed ones. In the review of Winget et al., all RP from the literature have been referenced to the SHE for sake of consistency, and the same mistake was reproduced.[31] Namazian et al. used a value of 4.60 V for SCE in acetonitrile,[32] whereas Roy et al. used the same value of 4.60 V for SHE in acetonitrile.[33] However, even if the reported absolute values in all these studies are fraught with systematic errors, the relative calculated RP within a series of compounds often correlate very well with experimental trends. For example, Roy et al. calculated the RP of a whole series of Fe dinuclear complexes and showed that B3LYP results correlate well with experimental trends within the series but require a consistent shift of −0.82 and −0.53 V to fit the experimental oxidation and reduction potentials respectively.[34] The calculated relative RPs should thus be well reproduced by DFT studies.

A way to remove systematic errors due to the uncertainty of the absolute potentials of the standard electrodes is the use of a suitable explicit reference redox couple also in the calculations. Roy et al. suggested to reference all RPs of transition-metal complexes to the calculated ARP of the ferricinium/ferrocene couple $[(C_5H_5)_2Fe^{III}]^+/[(C_5H_5)_2Fe^{II}]$ (Fc$^+$/Fc).[33] Indeed this redox couple is recommended by IUPAC as an internal standard for all electrochemical experiments.[27] However, it is noteworthy that the experimental RP of Fc$^+$/Fc is also dependent on the solvent and electrolyte conditions.[35] Konezny et al. proposed then to use internal reference redox couples complying with the following requirements:[36] i) The RP of the reference redox couple must be experimentally determined under the same conditions (solvent, electrolyte, working electrode, etc.) as for the complexes of interest. ii) the RP of the reference redox couple must be calculated under the same conditions (level of theory, solvent parameters, etc.) as for the complexes of interest. iii) The reference redox couple must involve a transition metal of the same row of the periodic table as for the complexes of interest. The RP is then calculated as

$$E^{\circ}(V/RRC) = E^{\circ}_{abs}(V) - E^{\circ}_{RRC}(V)$$

where $E^{\circ}$ is referenced to the reference redox couple (RRC), and $E^{\circ}_{RRC}$ is the calculated ARP of the RRC. The calculated $E^{\circ}$ can then be compared with the experimental $E^{\circ}$ referenced to the reference redox couple. The three constraints presented

above should effectively remove experimental or theoretical sources of systematic errors.

In our system of interest, the $Fc^+/Fc$ redox couple is a good candidate for the reference. Indeed the RP of $Fc^+/Fc$ has been measured as 0.460 V/SCE by Takahashi et al. under the same conditions as the measured RP of the $[(TMP^{+\bullet})Fe^{IV}(O)(L)]/$ $[(TMP)Fe^{IV}(O)(L)]$ couple (in dichloromethane at 213 K).[13] Moreover, the transition metal is the same in the RRC and the complexes of interest (i.e., iron). The first presented results will thus be the computed ARP of the $Fc^+/Fc$ couple.

## ■ RESULTS AND DISCUSSION

**Calculations of the ARP of the Reference Couple $Fc^+/$ Fc.** First, the ferricinium cation and ferrocene have been optimized in gas-phase with three functionals and B1 basis. Experimental and theoretical geometries of ferrocene are collected in Table 1. All calculated bond lengths are close to

**Table 1. Theoretical and Experimental[39] Bond Lengths in Ferrocene**

|  | B3LYP | BP86 | M06-L | expt |
|---|---|---|---|---|
| Fe−Cp[a] | 1.69 | 1.65 | 1.62 | 1.66 |
| Fe−C | 2.08 | 2.05 | 2.02 | 2.06 |
| C−C | 1.43 | 1.44 | 1.43 | 1.44 |
| C−H | 1.08 | 1.09 | 1.08 | 1.10 |

[a]Midpoint of Cp ring.

the experimental values, the largest discrepancy being 0.04 Å for the Fe−Cp and Fe−C bond lengths calculated with M06-L. Globally, BP86 gives the most accurate results since the geometry matches almost perfectly the experimental structure, in line with previous findings that BP86 tends to describe structures of 3D-metal complexes rather well,[37] in particular for ferrocene.[38]

The ARP calculated with the three functionals, the three basis sets, and the three solvation methods are reported in Table 2. A first obvious trend from the data is that the basis set

**Table 2. Calculated ARP (in V) of the Half-Reaction $Fc^+ +$ $e^- \rightarrow Fc$ in Dichloromethane**

|  | CPCM (UFF) | CPCM (Pauling) | SMD |
|---|---|---|---|
| B3LYP/B1 | 5.29 | 5.00 | 5.05 |
| B3LYP/B2 | 5.45 | 5.16 | 5.21 |
| B3LYP/B3 | 5.49 | 5.19 | 5.25 |
| BP86/B1 | 4.90 | 4.61 | 4.64 |
| BP86/B2 | 5.06 | 4.77 | 4.81 |
| BP86/B3 | 5.10 | 4.81 | 4.84 |
| M06-L/B1 | 4.81 | 4.51 | 4.57 |
| M06-L/B2 | 4.94 | 4.64 | 4.70 |
| M06-L/B3 | 4.94 | 4.64 | 4.71 |

of the lighter atoms has a noticeable influence on the RP. The RP increases when the basis set becomes larger. The difference reaches 0.20 V (i.e., ∼ 5 kcal/mol) between B1 and B3 for B3LYP and BP86. M06-L calculations are less dependent on the basis set since there is no difference between the B2 and B3 results. It is also noteworthy that the solvation method has a large influence on the computed RP. Although SMD and CPCM (with Pauling radii) give quite similar values (differences of 0.04−0.06 V, i.e. ∼ 1 kcal/mol), the use of the UFF radii changes the results dramatically. RPs calculated with

CPCM (UFF) differ from the ones calculated with CPCM (Pauling) by 0.30 V (i.e., ∼7 kcal/mol). These trends are reproduced for each functional. Finally, the nature of the functional has the largest influence on the calculated RP. B3LYP potentials are globally 0.40 V (i.e., ∼10 kcal/mol) and 0.50 V (i.e., ∼ 12 kcal/mol) higher than the ones computed with BP86 and M06-L, respectively. Roy et al. already observed these large differences between B3LYP and BP86 and attributed them to the amount of Hartree−Fock exchange in the two functionals.[33] In this article, Roy et al. computed the RP of the $Fc^+/Fc$ couple in three different solvents ($CH_3CN$, acetone, and DMSO) and referenced the potentials to the experimental SHE potentials measured in the three solvents. Thus they observed that the calculated potential of $Fc^+/Fc$ in $CH_3CN$ was better reproduced (exp. 0.65 V/SHE) with B3LYP (0.65 V/SHE) than with BP86 (0.20 V/SHE). On the other hand, the potentials of $Fc^+/Fc$ in acetone (DMSO) (exp. 0.72 V/SHE (0.67 V/SHE)) were better reproduced with BP86 (0.72 V/SHE (0.98 V/SHE)) than with B3LYP (1.16 V/SHE (1.41 V/SHE)). They noticed that a consistent shift in RP of 0.52 V (0.77 V) appeared for the acetone (DMSO) results versus the $CH_3CN$ results for each functional. However, they could not find the origin of this apparent systematic error in the calculations. It is noteworthy that the three used reference potentials were different (4.60 V, 4.13 V, and 3.83 V for SHE in $CH_3CN$, acetone, and DMSO, respectively) and that the differences between these reference potentials are 0.47 V (0.77 V) for acetone (DMSO) versus $CH_3CN$. These values reveal that the consistent shifts in RP between acetone (DMSO) and $CH_3CN$ were due to the use of these different references and that the calculated ARP of $Fc^+/Fc$ was not dependent on the solvent used in the continuum model (see Table 3).

**Table 3. ARP of the $Fc^+/Fc$ Couple in $CH_3CN$, Acetone, and DMSO, Calculated by Roy et al.[33]**

|  | exp. RP/ SHE | theor. RP/ SHE[a] | exp. ref. (SHE) | theor. ARP[b] |
|---|---|---|---|---|
| B3LYP/ $CH_3CN$ | 0.65 | 0.65 | 4.60 | 5.25 |
| B3LYP/acetone | 0.72 | 1.16 | 4.13 | 5.29 |
| B3LYP/DMSO | 0.67 | 1.41 | 3.83 | 5.24 |
| BP86/$CH_3CN$ | 0.65 | 0.20 | 4.60 | 4.80 |
| BP86/acetone | 0.72 | 0.72 | 4.13 | 4.85 |
| BP86/DMSO | 0.67 | 0.98 | 3.83 | 4.81 |

[a]Theoretical RPs computed by Roy et al. (6-311G** for C and H; SDD for Fe; PCM (UFF)). [b]Deduced values from the work of Roy et al.

The large difference between B3LYP and BP86 is almost 0.45 V in each case, but it is not possible to say which functional performs better. Since the experimental $E°$ are almost the same in the three solvents, and given that the SHE reference potentials are very different in the three solvents, the ARP of $Fc^+/Fc$ should be very different too in the three solvents. It is not clear if the experimental references are inaccurate, as they would imply excessively large differences on going from one solvent to another, or if the solvation effects are underestimated by the calculations. The experimental reference potentials could suffer from the complication of possible liquid junction potential between the aqueous electrode and the organic solvents. In order to remove both sources of errors, the method of Konezny et al. seems to be particularly promising.[36]

D

dx.doi.org/10.1021/ct400975w | J. Chem. Theory Comput. XXXX, XXX, XXX−XXX

Thus, the ARPs calculated with DFT depend strongly on the functional, the continuum model and the basis set of the lighter atoms (the effective core potential of iron should not have a large impact on the ARP, as it has been shown by Roy et al.[33]). The use of reference redox couples to calculate RPs is thus as relevant on the theoretical point of view as it is on the experimental one. Ideally, the RPs calculated with internal references should not depend on the level of theory as long as the reference redox couple and the complexes of interest are computed at the same level.

**Calculations on $[(TMP^{+\bullet})Fe^{IV}(O)(L)]$ and $[(TMP)Fe^{IV}(O)$-$(L)]$.** The only experimental structure reported for these complexes comes from the EXAFS spectra of $[(TMP^{+\bullet})$-$Fe^{IV}(O)(Cl^-)]$ and $[(TMP^{+\bullet})Fe^{IV}(O)(Br^-)]$ by Wolter et al.[40] $[(TMP^{+\bullet})Fe^{IV}(O)(Cl^-)]$ has thus been optimized in gas-phase with the three functionals and basis set B1. Bond lengths as well as both experimental[41] and theoretical Fe=O Raman stretching frequencies are presented in Table 4. BP86 reproduces the bond lengths and the stretching frequency better than B3LYP and M06-L, for which the Fe=O bond is calculated too short and too strong.

**Table 4. Calculated and Experimental Bond Lengths and Fe=O Raman Stretching Frequencies of $[(TMP^{+\bullet})Fe^{IV}(O)(Cl^-)]$**

|  | exp.[a] | B3LYP | BP86 | M06-L |
|---|---|---|---|---|
| d (Fe=O) | 1.66(1) | 1.634 | 1.658 | 1.648 |
| d (Fe−Cl) | 2.39(2) | 2.404 | 2.390 | 2.398 |
| d (Fe−N) | 1.99(1) | 2.023 | 1.993 | 2.015 |
| $\nu$ (Fe=O) | 801 | 885.1 | 825.9 | 844.8 |

[a]Distances and stretching frequencies from refs 40 and 41, respectively.

$[(TMP^{+\bullet})Fe^{IV}(O)(L)]$ was also optimized with other L ligands (L = none, $CH_2Cl_2$, Im, $ClO_4^-$, $CH_3CO_2^-$, $F^-$, $SCH_3^-$), and results are shown for the BP86 structures in Table 5. The

**Table 5. Calculated Bond Lengths and Fe=O Raman Stretching Frequencies of $[(TMP^{+\bullet})Fe^{IV}(O)(L)]$ and $[(TMP)Fe^{IV}(O)(L)]$ (in Parentheses) with BP86**

| L | d (Fe=O) | d (Fe−L) | $\nu$ (Fe=O) |
|---|---|---|---|
| none | 1.622 (1.627) | - (-) | 907.8 (899.9) |
| $CH_2Cl_2$ | 1.623 (1.628) | 3.014 (-)[a] | 905.5 (898.1) |
| Im | 1.643 (1.642) | 2.160 (2.196) | 863.0 (868.9) |
| $ClO_4^-$ | 1.644 (1.641) | 2.107 (2.197) | 843.9 (853.2) |
| $CH_3CO_2^-$ | 1.654 (1.657) | 2.044 (2.048) | 832.5 (834.4) |
| $Cl^-$ | 1.658 (1.660) | 2.390 (2.421) | 825.9 (827.1) |
| $F^-$ | 1.668 (1.671) | 1.868 (1.881) | 822.5 (817.7) |
| $SCH_3^-$ | 1.656 (1.680) | 2.502 (2.448) | 816.7 (777.7) |

[a]$CH_2Cl_2$ not bound for Cpd II.

Fe=O bond length as well as the Fe=O stretching frequency[42] give some insights about the influence of the sixth axial ligand. If the pristine five-coordinate complex (i.e., L = none) is taken as the reference, it is noteworthy that the solvent $CH_2Cl_2$ has no effect, whereas all the other ligands induce a *trans* influence by weakening and elongating the Fe=O bond. This phenomenon is also observable for Cpd II, $[(TMP)Fe^{IV}(O)(L)]$ (see values in parentheses in Table 5). The order in terms of *trans* influence importance is $SCH_3^- > F^-$ $> Cl^- > CH_3CO_2^- > ClO_4^- >$ Im.

**Calculations of the Redox Potential of the $[(TMP^{+\bullet})$-$Fe^{IV}(O)]/[(TMP)Fe^{IV}(O)]$ Couple.** All RPs will systematically be compared with the case where L = none. The calculated ARP of the $[(TMP^{+\bullet})Fe^{IV}(O)]/[(TMP)Fe^{IV}(O)]$ couple are presented in Table 6 with all different methods. It is

**Table 6. Calculated ARPs of $[(TMP^{+\bullet})Fe^{IV}(O)]/$ $[(TMP)Fe^{IV}(O)]^{a}$**

|  | CPCM (UFF) | CPCM (Pauling) | SMD |
|---|---|---|---|
| B3LYP/B1 | 5.31 (0.02) | 5.01 (0.01) | 5.06 (0.01) |
| B3LYP/B2 | 5.55 (0.10) | 5.25 (0.09) | 5.30 (0.09) |
| B3LYP/B3 | 5.59 (0.10) | 5.29 (0.10) | 5.34 (0.09) |
| BP86/B1 | 5.44 (0.54) | 5.19 (0.58) | 5.22 (0.58) |
| BP86/B2 | 5.63 (0.57) | 5.37 (0.60) | 5.40 (0.59) |
| BP86/B3 | 5.66 (0.56) | 5.41 (0.60) | 5.44 (0.60) |
| M06-L/B1 | 5.43 (0.62) | 5.18 (0.67) | 5.22 (0.65) |
| M06-L/B2 | 5.54 (0.60) | 5.29 (0.65) | 5.33 (0.63) |
| M06-L/B3 | 5.55 (0.61) | 5.30 (0.66) | 5.34 (0.63) |

[a]Calculated RPs of $[(TMP^{+\bullet})Fe^{IV}(O)]/[(TMP)Fe^{IV}(O)]$ referenced to the $Fc^+/Fc$ couple are presented in parentheses.

noteworthy that some trends observed for the $Fc^+/Fc$ couple appear for this system too, e.g. the influence of the basis set for the ligand atoms as well as the influence of the continuum model. Even the absolute differences between basis sets and continuum models (for example, 0.30 V between CPCM (UFF) and CPCM (Pauling)) are close to the ones observed with $Fc^+/Fc$, which justifies the approach of Konezny et al.[36] On the other hand, the differences between the three functionals observed for $Fc^+/Fc$ are rather less pronounced for the $[(TMP^{+\bullet})Fe^{IV}(O)]/[(TMP)Fe^{IV}(O)]$ system. As a consequence, the calculated RPs referenced to the $Fc^+/Fc$ couple present very large differences whether B3LYP or BP86/ M06-L are used (see Table 6). Since the experimental RPs for the $[(TMP^{+\bullet})Fe^{IV}(O)(L)]/[(TMP)Fe^{IV}(O)(L)]$ system are around 0.3−0.6 V/RRC,[13] the values calculated with B3LYP seem to be wrong, which would mean that the ARPs of the $Fc^+/Fc$ couple calculated with B3LYP are the origin of the error. For this reason, we will only focus on the BP86 results. It is noteworthy that the RPs calculated with each functional are very close irrespective of the basis set or continuum model. For example, with BP86, the maximum deviation is 0.06 V (between 0.54 and 0.60 V). This shows that the approach of Konezny et al.[36] works well, even if the errors due to the nature of the functional are not necessarily reproduced from one system to another, as it is the case here.

Only the results obtained with basis set B3 and the continuum model CPCM (UFF) will be presented for the other ligands L. The RP of the $[(TMP^{+\bullet})Fe^{IV}(O)]/[(TMP)$-$Fe^{IV}(O)]$ is computed to be 0.56 V/RRC at this level of theory. All the other results, including the B3LYP and M06-L ones, are presented in the Supporting Information.

**Calculations of the Redox Potentials of the $[(TMP^{+\bullet})$-$Fe^{IV}(O)(L)]/[(TMP)Fe^{IV}(O)(L)]$ Couples.** In order to compute the RPs of the $[(TMP^{+\bullet})Fe^{IV}(O)(L)]/[(TMP)Fe^{IV}(O)(L)]$ couples, it is important to have insights about the association energy of the ligand L to both $[(TMP^{+\bullet})Fe^{IV}(O)]$ and $[(TMP)Fe^{IV}(O)]$. The thermodynamic cycles used to calculate the association energies in solution are presented in Figure 4. According to these cycles, the association energy in solution is computed as
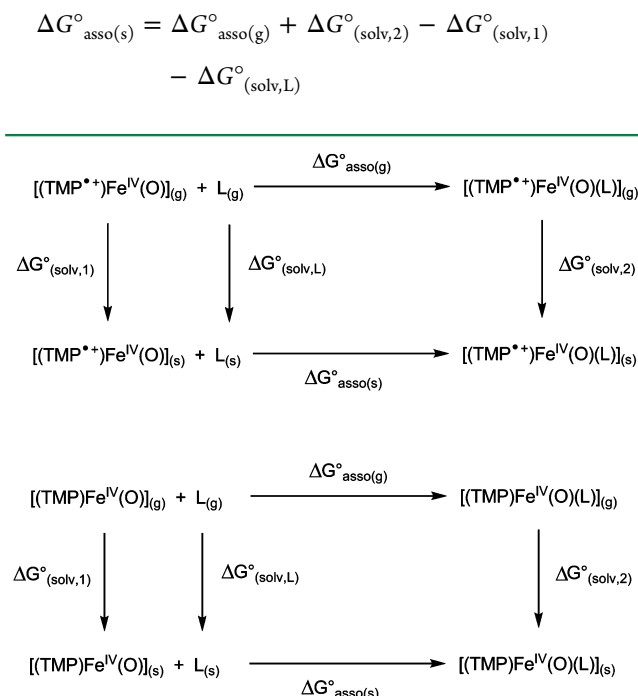
$$\Delta G^{\circ}{}_{asso(s)} = \Delta G^{\circ}{}_{asso(g)} + \Delta G^{\circ}{}_{(solv,2)} - \Delta G^{\circ}{}_{(solv,1)}$$
$$- \Delta G^{\circ}{}_{(solv,L)}$$



**Figure 4.** Thermodynamic cycles for the calculation of association energies in solution (top: oxidant, bottom: reductant).

The results are summarized in Table 7 for the BP86/B3/CPCM (UFF) level of theory.

**Table 7. Calculated Free Energies of Association (in kcal/mol) of the Ligands L with the Oxidant and the Reductant**

| L | $[(TMP^{+\bullet})Fe^{IV}(O)(L)]$ | $[(TMP)Fe^{IV}(O)(L)]$ |
|---|---|---|
| Im | −4.0 | +4.5 |
| $ClO_4^-$ | −2.2 | +11.2 |
| $CH_3CO_2^-$ | −13.6 | +6.6 |
| $Cl^-$ | −12.1 | +5.5 |
| $F^-$ | −27.7 | −9.8 |
| $SCH_3^-$ | −26.2 | 0 |

For the set of studied ligands, two different situations appear. Indeed, the association of L with $[(TMP^{+\bullet})Fe^{IV}(O)]$ is always found favorable, whereas the association of L with $[(TMP)Fe^{IV}(O)]$ is only favorable for $F^-$ (it is noteworthy that the association of L with $[(TMP)Fe^{IV}(O)]$ is always found favorable in terms of electronic energies, but not in terms of Gibbs energies, because of the entropic contribution). Thus, there are two half-reactions to consider in order to calculate the ARPs:

$$[(TMP^{+\bullet})Fe^{IV}(O)(L)] + e^- \rightarrow [(TMP)Fe^{IV}(O)(L)]$$

$$[(TMP^{+\bullet})Fe^{IV}(O)(L)] + e^- \rightarrow [(TMP)Fe^{IV}(O)] + L$$
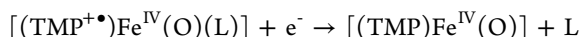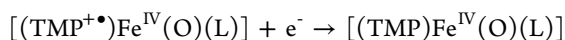
The first one is used for L = $F^-$, while the second one is used for all other ligands. For L = $F^-$, the ARP is thus calculated with the Born−Haber cycle of Figure 3. For the other ligands, the ARP is calculated with the cycle presented in Figure 5, as

$$\Delta G^{\circ}{}_{(s)} = \Delta G^{\circ}{}_{(g)} + \Delta G^{\circ}{}_{(solv,Red)} + \Delta G^{\circ}{}_{(solv,L)}$$
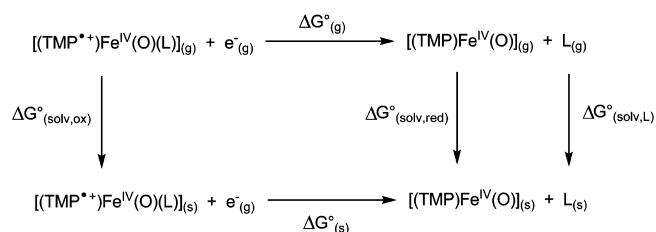$$- \Delta G^{\circ}{}_{(solv,Ox)}$$



**Figure 5.** Born−Haber cycle when L is not associated with the reductant.

The redox potentials calculated for the $[(TMP^{+\bullet})Fe^{IV}(O)(L)]/[(TMP)Fe^{IV}(O)] + L$ couples (and the $[(TMP^{+\bullet})Fe^{IV}(O)(F^-)]/[(TMP)Fe^{IV}(O)(F^-)]$ couple) are presented in Table 8. It is noteworthy that the calculated trend within the

**Table 8. Calculated Redox Potentials[a]**

| L | $E^{\circ}{}_{abs}$ (V) | $E^{\circ}$ (V/RRC) | $E^{\circ}{}_{exp}$ (V/RRC) |
|---|---|---|---|
| none | 5.66 | 0.56 | - |
| Im | 5.49 | 0.39 | 0.34 |
| $ClO_4^-$ | 5.57 | 0.47 | 0.42 |
| $CH_3CO_2^-$ | 5.07 | −0.03 | 0.58 |
| $Cl^-$ | 5.14 | 0.04 | 0.51 |
| $F^-$ | 4.89 | −0.21 | 0.50 |
| $SCH_3^-$ | 4.53 | −0.57 | - |

[a]First column: ARP. Second column: RP referenced to $Fc^+/Fc$. Third column: experimental RP referenced to $Fc^+/Fc$.

series is dramatically different from the experimental one. The order of calculated potentials is none > $ClO_4^-$ > Im > $Cl^-$ > $CH_3CO_2^-$ > $F^-$ > $SCH_3^-$. This can be directly deduced from the relative Gibbs energies of association of the L ligands (Table 7) with $[(TMP^{+\bullet})Fe^{IV}(O)]$ and $[(TMP)Fe^{IV}(O)]$ (see Figure 6). According to the work of Ogliaro et al.,[10a] the binding energies ordering is due to the combination of two effects: 1) the field effect, i.e. the negative charge of the axial ligand stabilizes the positive charge of the oxidant; 2) the quantum mechanical effect, which is mainly associated with the mixing of the orbitals of the ligand with the orbital located on the porphyrin ring; the quantum mechanical effect is larger when the axial ligand has strong σ- and π- donor abilities, as it is the case for $SCH_3^-$.

In order to eliminate probable issues with the methodology regarding this discrepancy,[43] other test calculations were carried out, namely 1) optimizations of complexes in the solvent, 2) addition of an explicit electrolyte species, and 3) addition of an explicit solvent molecule.

First, $[(TMP^{+\bullet})Fe^{IV}(O)(F^-)]$ and $[(TMP)Fe^{IV}(O)(F^-)]$ have been optimized in the continuum at the BP86/B1/SMD level of theory. The computed ARP is 4.42 V. For the single point SMD calculations on the gas-phase geometries, the computed ARP is 4.40 V. The optimization in solvent has thus no effect on the calculated value of the ARP. The addition of an electrolyte anion $ClO_4^-$ in a H-bonding interaction with the imidazole ligand in $[(TMP^{+\bullet})Fe^{IV}(O)(Im)]$ and $[(TMP)Fe^{IV}(O)(Im)]$ leads to an ARP of 5.44 V at the BP86/B3/CPCM(UFF) level of theory, in comparison with 5.49 V when no perchlorate is added. $ClO_4^-$ does not remain in the vicinity of the other complexes during the optimizations because of electrostatic repulsion with the negatively charged ligands. Finally, an explicit $CH_2Cl_2$ molecule was added to the system with L = $F^-$. An H-bond appears between $F^-$ and one hydrogen

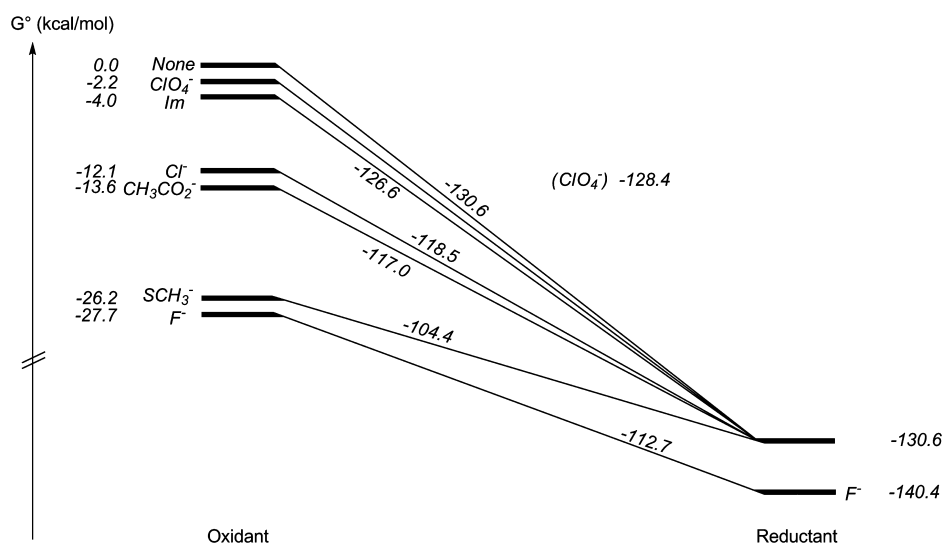**Figure 6.** Relative Gibbs energies of the association of L to the oxidant $[(TMP^{+\bullet})Fe^{IV}(O)]$ (on the left) and relative Gibbs energy of the association of $F^-$ to the reductant (on the right). The difference of energy between the oxidant and the reductant for each ligand L is related to the ARP of the corresponding redox couple by the conversion factor $1/F$ (with $F = 23.061$ kcal·mol$^{-1}$·V$^{-1}$).

atom of $CH_2Cl_2$. The ARP is calculated to be 4.70 V at the BP86/B1/CPCM(UFF) level versus 4.58 V when no implicit ligand is included. All these differences are clearly too small to make a difference in the computed trends, so these methodology issues should not be critical here.

**Orbital Energies.** Even though Koopmans' theorem formally only applies to Hartree−Fock calculations, Hamel et al. showed that in a similar vein Kohn−Sham orbital energies can provide fair approximations of ionization energies, certainly for the HOMO.[44] The RP of the $[(TMP^{+\bullet})Fe^{IV}(O)(L)/$ $[(TMP)Fe^{IV}(O)(L)]$ couple is directly related to the first ionization energy of $[(TMP)Fe^{IV}(O)(L)]$ (which is equal to the electron affinity of $[(TMP^{+\bullet})Fe^{IV}(O)(L)]$). Since the association of L with the reductant is always favorable in terms of electronic energy (but only favorable for L = $F^-$ in terms of Gibbs energy), it is thus relevant to compare the energy of the HOMO of $[(TMP)Fe^{IV}(O)(L)]$ with its ionization energy for each ligand L. Thus, the electronic energies of the half-reactions $[(TMP^{+\bullet})Fe^{IV}(O)(L)] + e^- \rightarrow [(TMP)Fe^{IV}(O)(L)]$ as well as the corresponding ionization energies in eV and the energies of the HOMOs of $[(TMP)Fe^{IV}(O)(L)]$ were calculated in gasphase and in solution and are reported in Table 9. The absolute values of the ionization energies do not match with $-E(HOMO)$, but the relative trends are perfect, both in gas-

phase and in solution, as can be seen in Figure 7. The relative energies of the HOMO orbital of Cpd II are thus a good estimation of the relative ionization energies of Cpd II (or electron affinities of Cpd I).

**Variation of Substituents on the Porphyrin Ring.** Takahashi et al. showed that the addition of electron-withdrawing substituents on the meso-positions of the porphyrin ring leads to higher redox potentials.[13] We calculated the RP of the $[(TDCP^{+\bullet})Fe^{IV}(O)(ClO_4^-)]/[(TDCP)Fe^{IV}(O)]$ $+ ClO_4^-$ and $[(TPFP^{+\bullet})Fe^{IV}(O)(ClO_4^-)]/[(TPFP)Fe^{IV}(O)] +$



**Table 9. Electronic Energies $\Delta E$ of the Half-Reaction $[(TMP^{+\bullet})Fe^{IV}(O)(L)] + e^- \rightarrow [(TMP)Fe^{IV}(O)(L)]$, Ionization Energies IE of $[(TMP)Fe^{IV}(O)(L)]$, and $-E(HOMO)$ of $[(TMP)Fe^{IV}(O)(L)]^a$**

| L | $\Delta E$ (kcal/mol) | IE (eV) | $-E(HOMO)$ (eV) |
|---|---|---|---|
| none | −148.5 (−131.2) | 6.44 (5.69) | 5.12 (5.39) |
| Im | −137.7 (−122.0) | 5.97 (5.29) | 4.64 (4.97) |
| $ClO_4^-$ | −85.8 (−116.7) | 3.72 (5.06) | 2.41 (4.70) |
| $CH_3CO_2^-$ | −77.1 (−109.7) | 3.34 (4.76) | 2.00 (4.45) |
| $Cl^-$ | −77.6 (−112.5) | 3.37 (4.88) | 2.01 (4.51) |
| $F^-$ | −76.1 (−111.7) | 3.30 (4.85) | 2.01 (4.51) |
| $SCH_3^-$ | −68.8 (−103.9) | 2.98 (4.51) | 1.59 (4.20) |

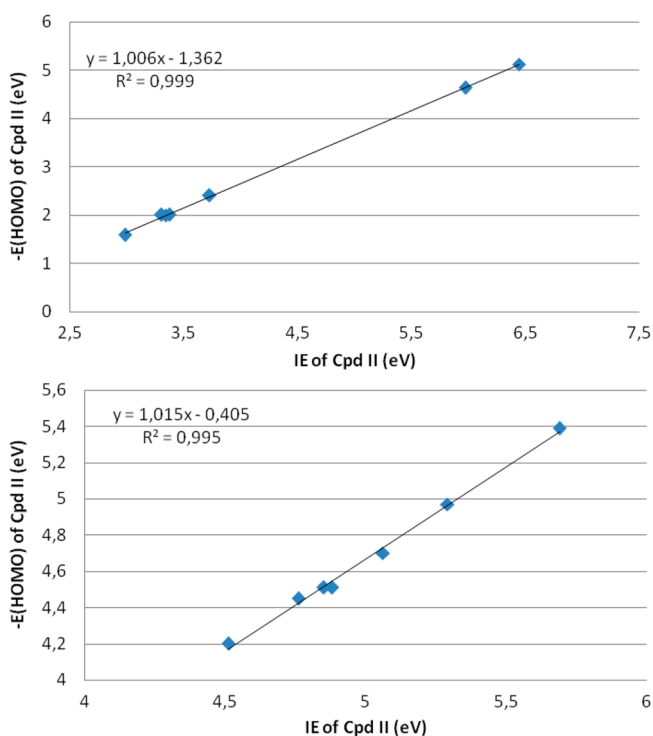$^a$Values computed in solution (CPCM(UFF), dichloromethane) are presented in parentheses.

**Figure 7.** Correlation diagrams of the calculated ionization energies of $[(TMP)Fe^{IV}(O)(L)]$ vs the calculated $-E(HOMO)$ of $[(TMP)Fe^{IV}(O)(L)]$, in gas-phase (top) and solution (bottom).

$ClO_4^-$ couples (with TDCP = tris(2,6-dichorophenyl)-porphyrinate and TPFP = tris(pentafluorophenyl)porphyrinate; see Figure 2 for formula). The results correlate quite well with experiments (0.47, 0.73, and 0.91 V/RRC versus 0.42, 0.815, and 0.93 V/RRC experimentally, for TMP, TDCP, and TPFP, respectively). The discrepancy for TDCP must be due to the fact that the RP was measured at −35 °C, and so the RP of $Fc^+/Fc$ should differ from the one measured at −60 °C. Thus 0.815 V/RRC is only an estimation of the RP for the TDCP complex. The effect of the electron-withdrawing substituents on the redox potential of this type of complexes has already been rationalized by Fujii.[45] It is noteworthy that the theory agrees very well with experiment when the axial ligand is $ClO_4^-$.

**Discussion.** The experimental order of the RPs is $CH_3CO_2^- > Cl^- > F^- > ClO_4^- > Im$, i.e. totally different from the computed one and, actually, difficult to rationalize. A strongly coordinating anionic ligand such as $F^-$ should stabilize the positively charged oxidant more strongly than a neutral one and should thus produce a smaller RP than the neutral ligand Im, as emerging, in fact, from the computations. The reason for this apparent discrepancy between experiment and theory (and chemical intuition) is not fully clear at present.

Assuming that all peaks have been correctly assigned and none have been missed, the observed trend in the RPs may not necessarily reflect the intrinsic redox properties of the octahedral porphyrin complexes but may rather be related to the specific composition of each solution under the experimental conditions. In all cases, the electrolyte [n-Bu$_4$N][ClO$_4$] is present, presumably in excess, and more complex equilibria than those considered here (Figures 3 and 4) may be involved. It is noteworthy that, using the pristine $Fc^+/Fc$ couple as RRC {$E°$ (V/RRC) data in Table 8}, computed and experimental RPs agree quite well for L = Im and $ClO_4^-$. Adding anionic ligands does not result in a decrease of the RP, as predicted, but rather in an increase, i.e. approaching the value computed for L = none. It might be that an increase of the ionic strength of the solution concomitant with addition of the ligands could disfavor formation of the $[(TMP^{+•})Fe^{IV}(O)(L)]$ adducts and increase the contributions from the pristine $[(TMP^{+•})Fe^{IV}(O)]/[(TMP)Fe^{IV}(O)]$ couple. The computed association energies with the oxidant for L = $CH_3CO_2^-$, $Cl^-$, and, in particular, $F^-$ (Table 7) would appear rather large to be counteracted by an increased ionic strength, but it should be kept in mind that these are results from simple continuum models, which may not always be quantitatively accurate.[46] Explicit solvation in a dynamic ensemble should be included in the calculations in order to study the speciation of the target complex under realistic conditions; however, such an effort is beyond the scope of the present paper.[47]

## CONCLUSION

We have computed the redox potentials of the $[(TMP^{+•})Fe^{IV}(O)(L)]/[(TMP)Fe^{IV}(O)(L)]$ couple for L = none, Im, $ClO_4^-$, $CH_3CO_2^-$, $Cl^-$, $F^-$ and $SCH_3^-$. The calculations show that the system with L = none presents the highest redox potential of the series. Each ligand L tends to stabilize the positively charged oxidant more than the neutral reductant and thus to decrease the redox potential of the couple. The theoretical ordering is L = none > $ClO_4^-$ > Im > $Cl^-$ > $CH_3CO_2^-$ > $F^-$ > $SCH_3^-$. These results agree very well with previous theoretical calculations that showed that the electron affinity of Cpd I is smaller when the sixth axial ligand is

negatively charged.[10] Moreover, the relative ionization energies of Cpd II can be estimated via its relative HOMO energies. These results are in disagreement with the experiments from Takahashi et al. showing that the coordination of a negative ligand shifts the redox potential upward.[13] The reason for this discrepancy is not clear. Perhaps an increase of the ionic strength of the solution disfavors the formation of the $[(TMP^{+•})Fe^{IV}(O)(L)]$ adducts. If this is the case, the experimental results should not correspond to the redox potentials of the $[(TMP^{+•})Fe^{IV}(O)(L)]/[(TMP)Fe^{IV}(O)(L)]$ couples. In a theoretical point of view, we demonstrated that the calculated absolute redox potentials are very dependent on the nature of the functional, the size of the basis set, and the nature of the continuum model. Some of these systematic errors (e.g., the size of the basis set and the continuum model) can be minimized by using an internal reference, like the absolute redox potential of $Fc^+/Fc$. However, the prediction of RPs can lead to very different results according to the nature of the functional (hybrid-GGA versus GGA in particular), even when using an internal reference.

## ASSOCIATED CONTENT

**Ⓢ Supporting Information**

Electronic energies and Gibbs energies, as well as Cartesian coordinates and absolute redox potentials calculated with all different methods. This material is available free of charge via the Internet at http://pubs.acs.org.

## AUTHOR INFORMATION

**Corresponding Author**

*E-mail: buehl@st-andrews.ac.uk.

**Notes**

The authors declare no competing financial interest.

## ACKNOWLEDGMENTS

## REFERENCES

(1) (a) Dunford, H. B.; Stillman, J. S. *Coord. Chem. Rev.* **1976**, *19*, 187−251. (b) Dunford, H. B. *Heme Peroxidases*; Wiley-VCH: New York, 1999. (c) Schonbaum, G. R.; Chance, B. *In The Enzymes*; Boyer, P. D., Ed.; Academic Press: New York, 1976; Vol. 13, pp 363−408.

(2) (a) de Montellano, P. O. *Cytochrome P450: Structure, Mechanism, and Biochemistry*, 3rd ed.; Kluwer Academic: New York, 2005. (b) Denisov, I. G.; Makris, T. M.; Sligar, S. G.; Schlichting, I. *Chem. Rev.* **2005**, *105*, 2253−2277. (c) Meunier, B.; de Visser, S. P.; Shaik, S. *Chem. Rev.* **2004**, *104*, 3947−3980. (d) Shaik, S.; Kumar, D.; de Visser, S. P.; Altun, A.; Thiel, W. *Chem. Rev.* **2005**, *105*, 2279−2328.

(3) Sono, M.; Roach, M. P.; Coulter, E. D.; Dawson, J. H. *Chem. Rev.* **1996**, *96*, 2841−2887.

(4) Kersten, P. J.; Kalyanaraman, B.; Hammel, K. E.; Reinhammar, B.; Kirk, T. K. *Biochem. J.* **1990**, *268*, 475−480.

(5) Hayashi, Y.; Yamasaki, I. *J. Biol. Chem.* **1979**, *254*, 9101−9106.

(6) Conroy, C. W.; Tyma, P.; Daum, P. H.; Erman, J. E. *Biochim. Biophys. Acta* **1978**, *537*, 62−69.

(7) Gross, Z.; Nimri, S. *Inorg. Chem.* **1994**, *33*, 1731−1732.

(8) Kang, Y.; Chen, H.; Jeong, Y. J.; Lai, Z.; Bae, E. H.; Shaik, S.; Nam, W. *Chem.—Eur. J.* **2009**, *15*, 10039−10046.

(9) (a) Rydberg, P.; Sigfridsson, E.; Ryde, U. *J. Biol. Inorg. Chem.* **2004**, *9*, 203−223. (b) Dey, A.; Jiang, Y.; de Montellano, P. O.;

Hodgson, K. O.; Hedman, B.; Solomon, E. I. *J. Am. Chem. Soc.* **2009**, *131*, 7869−7878.

(10) (a) Ogliaro, F.; de Visser, S. P.; Shaik, S. *J. Inorg. Biochem.* **2002**, *91*, 554−567. (b) Wang, R.; de Visser, S. P. *J. Inorg. Biochem.* **2007**, *101*, 1464−1472. (c) Kumar, D.; de Visser, S. P.; Sharma, P. K.; Derat, E.; Shaik, S. *J. Biol. Inorg. Chem.* **2005**, *10*, 181−189.

(11) (a) Kumar, D.; Sastry, G. N.; de Visser, S. P. *J. Phys. Chem. B* **2012**, *116*, 718−730. (b) de Visser, S. P. *J. Am. Chem. Soc.* **2010**, *132*, 1087−1097.

(12) Takahashi, A.; Yamaki, D.; Ikemura, K.; Kurahashi, T.; Ogura, T.; Hada, M.; Fujii, H. *Inorg. Chem.* **2012**, *51*, 7296−7305.

(13) Takahashi, A.; Kurahashi, T.; Fujii, H. *Inorg. Chem.* **2011**, *50*, 6922−6928.

(14) Frisch, M. J.; Trucks, G. W.; Schlegel, H. B.; Scuseria, G. E.; Robb, M. A.; Cheeseman, J. R.; Scalmani, G.; Barone, V.; Mennucci, B.; Petersson, G. A.; Nakatsuji, H.; Caricato, M.; Li, X.; Hratchian, H. P.; Izmaylov, A. F.; Bloino, J.; Zheng, G.; Sonnenberg, J. L.; Hada, M.; Ehara, M.; Toyota, K.; Fukuda, R.; Hasegawa, J.; Ishida, M.; Nakajima, T.; Honda, Y.; Kitao, O.; Nakai, H.; Vreven, T.; Montgomery, J. A., Jr.; Peralta, J. E.; Ogliaro, F.; Bearpark, M.; Heyd, J. J.; Brothers, E.; Kudin, K. N.; Staroverov, V. N.; Kobayashi, R.; Normand, J.; Raghavachari, K.; Rendell, A.; Burant, J. C.; Iyengar, S. S.; Tomasi, J.; Cossi, M.; Rega, N.; Millam, J. M.; Klene, M.; Knox, J. E.; Cross, J. B.; Bakken, V.; Adamo, C.; Jaramillo, J.; Gomperts, R.; Stratmann, R. E.; Yazyev, O.; Austin, A. J.; Cammi, R.; Pomelli, C.; Ochterski, J. W.; Martin, R. L.; Morokuma, K.; Zakrzewski, V. G.; Voth, G. A.; Salvador, P.; Dannenberg, J. J.; Dapprich, S.; Daniels, A. D.; Farkas, Ö.; Foresman, J. B.; Ortiz, J. V.; Cioslowski, J.; Fox, D. J. *Gaussian 09*, Revision A.02; Gaussian, Inc.: Wallingford, CT, 2009.

(15) (a) Becke, A. D. *J. Chem. Phys.* **1993**, *98*, 5648−5652. (b) Lee, C.; Yang, W.; Parr, R. G. *Phys. Rev. B* **1988**, *37*, 785−789.

(16) (a) Becke, A. D. *Phys. Rev. A* **1988**, *38*, 3098−3100. (b) Perdew, J. P. *Phys. Rev. B* **1986**, *33*, 8822−8824.

(17) Zhao, Y.; Truhlar, D. G. *J. Chem. Phys.* **2006**, *125*, 194101/1−18.

(18) Dolg, M.; Wedig, U.; Stoll, H.; Preuss, H. *J. Chem. Phys.* **1987**, *86*, 866−872.

(19) Hehre, W. J.; Ditchfield, R.; Pople, J. A. *J. Chem. Phys.* **1972**, *56*, 2257−2261.

(20) (a) Edinger, S. R.; Cortis, C.; Shenkin, P. S.; Friesner, R. A. *J. Phys. Chem. B* **1997**, *101*, 1190−1197. (b) Friedrichs, M.; Zhou, R. H.; Edinger, S. R.; Friesner, R. A. *J. Phys. Chem. B* **1999**, *103*, 3057−3061. (c) Marten, B.; Kim, K.; Cortis, C.; Friesner, R. A.; Murphy, R. B.; Ringnalda, M. N.; Sitkoff, D.; Honig, B. *J. Phys. Chem.* **1996**, *100*, 11775−11788.

(21) Rashin, A. A.; Honig, B. *J. Phys. Chem.* **1985**, *89*, 5588−5593.

(22) Barone, V.; Cossi, M. *J. Phys. Chem. A* **1998**, *102*, 1995−2001.

(23) Marenich, A. V.; Cramer, C. J.; Truhlar, D. G. *J. Phys. Chem. B* **2009**, *113*, 6378−6396.

(24) Derat, E.; Cohen, S.; Shaik, S.; Altun, A.; Thiel, W. *J. Am. Chem. Soc.* **2005**, *127*, 13611−13621.

(25) (a) Li, J.; Fisher, C. L.; Chen, J. L.; Bashford, D.; Noodleman, L. *Inorg. Chem.* **1996**, *35*, 4694. (b) Tavernelli, I.; Vuilleumier, R.; Sprik, M. *Phys. Rev. Lett.* **2002**, *88*, 213002.

(26) (a) Trasatti, S. *Pure Appl. Chem.* **1986**, *58*, 955−966. (b) Kelly, C. P.; Cramer, C. J.; Truhlar, D. G. *J. Phys. Chem. B* **2006**, *110*, 16066−16081. (c) Kelly, C. P.; Cramer, C. J.; Truhlar, D. G. *J. Phys. Chem. B* **2007**, *111*, 408−422. (d) Fawcett, W. R. *Langmuir* **2008**, *24*, 9868−9875.

(27) Gritzner, G.; Kuta, J. *Pure Appl. Chem.* **1984**, *56*, 461−466.

(28) (a) Winget, P.; Weber, E. J.; Cramer, C. J.; Truhlar, D. G. *Phys. Chem. Chem. Phys.* **2000**, *2*, 1231−1239. (b) Patterson, E. V.; Cramer, C. J.; Truhlar, D. G. *J. Am. Chem. Soc.* **2001**, *123*, 2025−2031.

(29) Baik, M. H.; Friesner, R. A. *J. Phys. Chem. A* **2002**, *106*, 7407−7412.

(30) Holland, J. P.; Green, J. C.; Dilworth, J. R. *Dalton Trans.* **2006**, 783−794.

(31) Winget, P.; Cramer, C. J.; Truhlar, D. G. *Theor. Chem. Acc.* **2004**, *112*, 217−227.

(32) Namazian, M.; Lin, C. Y.; Coote, M. L. *J. Chem. Theory Comput.* **2010**, *6*, 2721−2725.

(33) Roy, L. E.; Jakubikova, E.; Guthrie, M. G.; Batista, E. R. *J. Phys. Chem. A* **2009**, *113*, 6745−6750.

(34) Roy, L. E.; Batista, E. R.; Hay, P. J. *Inorg. Chem.* **2008**, *47*, 9228−9237.

(35) (a) Kuwana, T.; Bublitz, D. E.; Hoh, G. *J. Am. Chem. Soc.* **1960**, *82*, 5811−5817. (b) Chang, D.; Malinski, T.; Ulman, A.; Kadish, K. M. *Inorg. Chem.* **1984**, *23*, 817−824. (c) Chang, J. P.; Fung, E. Y.; Curtis, J. C. *Inorg. Chem.* **1986**, *25*, 4233−4241. (d) Connelly, N. G.; Geiger, W. E. *Chem. Rev.* **1996**, *96*, 877−910.

(36) Konezny, S. J.; Doherty, M. D.; Luca, O. R.; Crabtree, R. H.; Soloveichik, G. L.; Batista, V. S. *J. Phys. Chem. C* **2012**, *116*, 6349−6356.

(37) Bühl, M.; Kabrede, H. *J. Chem. Theory Comput.* **2006**, *2*, 1282−1290.

(38) Bühl, M.; Malkina, O. L.; Malkin, V. G. *Helv. Chim. Acta* **1996**, *79*, 742−754.

(39) Haaland, A. *Acc. Chem. Res.* **1979**, *12*, 415.

(40) Wolter, T.; Meyer-Klaucke, W.; Müther, M.; Mandon, D.; Winkler, H.; Trautwein, A. X.; Weiss, R. *J. Inorg. Biochem.* **2000**, *78*, 117−122.

(41) Czarnecki, K.; Nimri, S.; Gross, Z.; Proniewicz, L. M.; Kincaid, J. R. *J. Am. Chem. Soc.* **1996**, *118*, 2929−2935.

(42) Raman stretching frequencies have long been used to probe the nature of the Fe=O bond, cf. ref 41; we note that our $\nu$(Fe=O) values computed for $[(TMP^{+\bullet})Fe^{IV}(O)(L)]$, 844 cm$^{-1}$, 826 cm$^{-1}$, and 823 cm$^{-1}$ for L = ClO$_4$, Cl, and F, respectively, fit reasonably well to the experimental findings in that paper (835 cm$^{-1}$, 801 cm$^{-1}$, and 801 cm$^{-1}$, respectively), even without scaling. Our computed values are in line with previous DFT data for model complexes in the literature (see e.g. ref 11a and the following: Ohta, T.; Matsuura, K.; Yoshizawa, K.; Morishima, I. *J. Inorg. Biochem.* **2000**, *82*, 141−152.

(43) In this context we note that trends in gas-phase electron affinities of Fe(III) porphyrins ( Chen, H. L.; Ellis, P. E.; Wijesekera, T.; Hagan, T. E.; Groh, S. E.; Lyons, J. E.; Ridge, D. P. *J. Am. Chem. Soc.* **1994**, *116*, 1086−1089 ) are well reproduced at our level, see Figure in the SI.

(44) Hamel, S.; Duffy, P.; Casida, M. E.; Salahub, D. R. *J. Electron Spectrosc. Relat. Phenom.* **2002**, *123*, 345−363.

(45) (a) Fujii, H. *J. Am. Chem. Soc.* **1993**, *115*, 4641−4648. (b) Fujii, H. *Coord. Chem. Rev.* **2002**, 51−60.

(46) Bühl, M.; Sieffert, N.; Wipff, G. *Chem. Phys. Lett.* **2009**, *467*, 287−293.

(47) Note that also redox potentials themselves have been modeled from first-principles molecular dynamics simulations, see: Costanzo, F.; Sulpizi, M.; Della Valle, R. G.; Sprik, M. *J. Chem. Phys.* **2011**, *134*, 244508-1−244508-21.